Mathematical Modelling and Numerical Simulation with Applications, 2022, 2(3), 164–176

https://www.mmnsa.org
ISSN Online: 2791-8564 / Open Access
https://doi.org/10.53391/mmnsa.2022.013

RESEARCH PAPER

Stability characterization of a fractional-order viral system with the non-cytolytic immune assumption

Mouhcine Naim [1,†], Yassine Sabbar [2,†,*] and Anwar Zeb [3,†]

[1]Laboratory of Analysis, Modeling and Simulation, Department of Mathematics and Computer Science, Faculty of Sciences Ben M'sik, Hassan II University, Casablanca, Morocco, [2]LPAIS Laboratory, Faculty of Sciences Dhar El Mahraz, Sidi Mohamed Ben Abdellah University, Fez, Morocco, [3]Department of Mathematics, COMSATS University Islamabad, Abbottabad Campus, Abbottabad 22060, Khyber Pakhtunkhwa, Pakistan

*Corresponding Author
†naimmouhcine2013@gmail.com (Mouhcine Naim); yassine.sabbar@usmba.ac.ma (Yassine Sabbar); anwar@cuiatd.edu.pk (Anwar Zeb)

Abstract

This article deals with a Caputo fractional-order viral model that incorporates the non-cytolytic immune hypothesis and the mechanism of viral replication inhibition. Firstly, we establish the existence, uniqueness, non-negativity and boundedness of the solutions of the proposed viral model. Then, we point out that our model has the following three equilibrium points: equilibrium point without virus, equilibrium state without immune system, and equilibrium point activated by immunity with humoral feedback. By presenting two critical quantities, the asymptotic stability of all said steady points is examined. Finally, we examine the finesse of our results by highlighting the impact of fractional derivatives on the stability of the corresponding steady points.

Key words: Viral model; non-cytolytic; immunity; fractional-order formulation; stability
AMS 2020 Classification: 26A33; 34A08; 45M10

1 Introduction

Mathematical modeling has become necessary to comprise our world and to study phenomena on time and space scales that are difficult to scope empirically [1]. Mathematics applied in virology seeks to investigate the interactions of viruses with the biological environment and their powerful influence on living organisms, both plants and animals. Viruses are scrutinized at different scales: molecular, cellular, in the body and, in the case of an epidemic, in the ecosystem or society as a whole [2]. Virological modeling also examines and models the spread of viruses at the population level. It starts from when they cross species barriers, until policy measures are put in place to reduce and treat disease. At this scale, the humanities can be called in as reinforcements. Specifically, it concentrates on structures, diffusion, dynamics, and immune capabilities of infections [3]. The blending of mathematical tools with virology pursues to predict the long-run attitude of a virus under certain conditions in order to help eradicate or control the infection. In terms of scientific research, the description of virus-cell interactions with different types of immune responses is a rich subject of interest for many researchers [4]. Thus, a number of studies have been devoted to the analysis of viral systems with a specific immune response combining humoral and cellular immunizations [5]. These two characteristics are types of adaptive immune reactions that permit the human organism to safeguard itself from threatening agents such as bacterial microorganisms, viruses and toxins, in a targeted way.

➤ **Received:** 29.07.2022 ➤ **Revised:** 22.09.2022 ➤ **Accepted:** 24.09.2022 ➤ **Published:** 25.09.2022

Recovery from infected cells is an important hypothesis along with the immune response. For this reason, it is appropriate to propose a viral model including the healing average of damaging cells employing the non-cytolytic immune feedback under humoral resistance. On the other hand, the host immune response during viral infection can be usually splitted into lytic and non-lytic elements [6], where the lytic elements kill the damaged cells, while the non-lytic elements prohibit viral replication through soluble media produced by immune cells. For example, in the case of SARS-CoV-2 infection, some authors have considered target cell models by proposing a framework with lytic and non-lytic immune responses to understand virus spread within the human body [7]. The human immune system consists of both innate and adaptive immune responses. While the adaptive immune system is quick and efficient in targeting invasions by previously encountered pathogens, its role in host defense in the early days of a new infection is secondary to the innate immune system. Motivated by these facts, Dhar et al. [4] exhibited the following viral system with non-cytolytic immune assumption:

$$\begin{cases} \mathbf{U}'(t) = \varphi - \mathfrak{h}_1\mathbf{U}(t) - \mathfrak{b}\mathbf{U}(t)\mathbf{Y}(t)\overbrace{(1+q\mathbf{W}(t))^{-1}}^{\text{Inhibition rate}} + \xi\mathbf{X}(t), \\ \mathbf{X}'(t) = \mathfrak{b}\mathbf{U}(t)\mathbf{Y}(t)(1+q\mathbf{W}(t))^{-1} - \mathfrak{h}_2\mathbf{X}(t) - \xi\mathbf{X}(t), \\ \mathbf{Y}'(t) = k\mathbf{X}(t) - \mathfrak{h}_3\mathbf{Y}(t) - p\mathbf{Y}(t)\mathbf{W}(t), \\ \mathbf{W}'(t) = c\mathbf{Y}(t)\mathbf{W}(t) - \mathfrak{h}_4\mathbf{W}(t), \end{cases} \tag{1}$$

with positive started data. Here, **U**, **X**, **Y** and **W** indicate in that order, susceptible uninfected cells, infected cells, free virus and B lymphocytes (cells used in the humoral immune process of the adaptive immune system). Regarding the positive parameters of system (1), φ indicates the inflow of **U** cells, k designates the produce ratio of **Y**, c is the growth rate of B lymphocytes, $\mathfrak{h}_1$, $\mathfrak{h}_2$, $\mathfrak{h}_3$ and $\mathfrak{h}_4$ are the natural mortality rates of **U**, **X**, **Y** and **W** cells respectively, p is the neutralizing rate of antibodies produced by B cells, ξ is the healing rate of infected cell due to the antiviral activity, and $\mathfrak{b}$ is the contamination rate. The expression $(1+q\mathbf{W})$ designates the rate at which the non-lytic process prevents viral growth, where q is the non-lytic force. To facilitate the understanding of the rest of this article, we summarize the transfer mechanisms of the model mentioned above by the diagram shown in Figure 1.

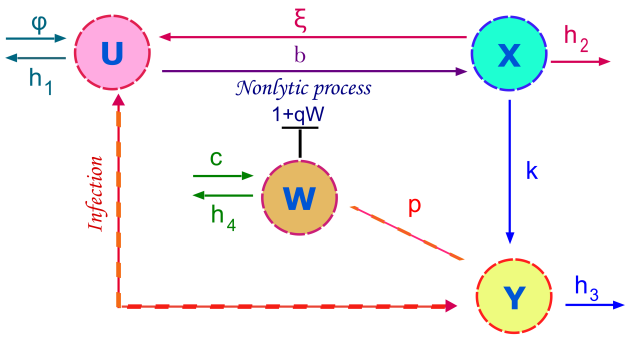

Figure 1. *Compartment diagram of the viral system* (1).

In [4], the authors established the steady points of system (1) and studied their asymptotic stability. Specifically, they provided the critical value between the disappearance and continuation of the infection. The results obtained in [4] are interesting and help us to understand the long term of the infection under some local characteristics of the classical order derivative. This type of mathematical formulation has certain limits, and the system (1) can be improved and updated by considering the fractional framework.

Fractional derivatives is a generalization of the integer order derivative to an arbitrary order, which is originated from the L'Hospital letter to Leibniz discussing the meaning of the derivative or what does the derivative of order $\frac{1}{2}$ or $\sqrt{2}$ of a function mean in 1695. Several definitions of fractional derivatives have been introduced. Among them, the Riemann–Liouville and Caputo's derivative are widely used in the literature. The fractional order derivative used in this paper is in the sense of Caputo definition, which is a modification of the Riemann-Liouville integral definition, and has the advantage that the initial values for fractional differential equations with Caputo derivatives take the same form as that for integer order differential equations [8, 9, 10]. Also, another advantage of this definition is that the Caputo derivative of a constant is zero. Memory effect is an essential characteristic of fractional-order derivatives which made fractional calculus and its applications widely used in many fields of science and engineering [11, 12, 13, 14, 15, 16, 17]. Obviously, this feature is very relevant for modeling the spread of infections [18, 19, 20, 21, 22, 23, 24]. For this reason, many researchers have adopted this analytical vision [25, 26, 27, 28, 29, 30, 31]. In [32], the authors derived a non-integer order system for the co-infection mechanisms. They inferred that the fractional formulation matches real data of certain viral problems. Analytically, they examined the stability property of the proposed viral model. To model the virological memory effects, the authors in [33], presented a fractional order viral model. They analyzed the long-term dynamics of the constructed model. As a real-world application, the authors in [34], proposed a fractional feeding system to illustrate the complexity of the spread of COVID-19. They presented an advanced analysis by discussing the attitude of viral propagation phenomena. In

accordance with the above arguments and works, we improve system (1) by using the fractional formulation as follows:

$$\begin{cases} {}_0^{\mathcal{C}}\mathbb{F}^{\sigma}\mathbf{U}(t) = & \varphi - \mathfrak{h}_1\mathbf{U}(t) - \mathfrak{b}\mathbf{U}(t)\mathbf{Y}(t)\big(1+q\mathbf{W}(t)\big)^{-1} + \xi\mathbf{X}(t), \\ {}_0^{\mathcal{C}}\mathbb{F}^{\sigma}\mathbf{X}(t) = & \mathfrak{b}\mathbf{U}(t)\mathbf{Y}(t)\big(1+q\mathbf{W}(t)\big)^{-1} - \mathfrak{h}_2\mathbf{X}(t) - \xi\mathbf{X}(t), \\ {}_0^{\mathcal{C}}\mathbb{F}^{\sigma}\mathbf{Y}(t) = & k\mathbf{X}(t) - \mathfrak{h}_3\mathbf{Y}(t) - p\mathbf{Y}(t)\mathbf{W}(t), \\ {}_0^{\mathcal{C}}\mathbb{F}^{\sigma}\mathbf{W}(t) = & c\mathbf{Y}(t)\mathbf{W}(t) - \mathfrak{h}_4\mathbf{W}(t), \end{cases} \tag{2}$$

where ${}_0^{\mathcal{C}}\mathbb{F}^{\sigma}$ is the Caputo fractional derivative and $\sigma \in (0,1]$ is its related order. The Caputo fractional derivative of order $\sigma \in (0,1]$ for a function $\mathfrak{f} \in \mathcal{C}(\mathbb{R}_+,\mathbb{R})$ is expressed as follows [35]:

$${}_0^{\mathcal{C}}\mathbb{F}^{\sigma}\mathfrak{f}(t) = \frac{1}{\Gamma(1-\sigma)}\int_0^t (t-s)^{-\sigma}\mathfrak{f}'(s)ds,$$

where Γ is the Gamma function and $\Gamma(\sigma) = \int_0^{\infty} t^{\sigma-1}e^{-t}dt$.

Note that, the fractional order formulation (2) is converted to ordinary differential equations system when $\sigma = 1$. Therefore, the model studied in [4] is a special case of system (1) when $\sigma = 1$.

The axial problematic of this research is to explore some long-run characteristics of the viral system (2) which adopts the non-integer order derivative. It is well known that stability analysis is an important property of dynamical systems. It provides a good overview of the long term of the studied phenomenon. Unlike classical investigations, in this survey, we concentrate on exploring the influence of fractional derivative on said features; and this is the main part of our contribution.

The remaining of this article is structured as follows: we begin in Section 2 by proving the well-posedness of our enhanced model in the sense that it has a unique nonnegative and bounded solution, defining the steady points $\mathbb{S}^{\circ}$, $\mathbb{S}_1^{\star}$, $\mathbb{S}_2^{\star}$ of system (2) and their related critical quantities $\mathcal{T}_{\circ}$ and $\mathcal{T}_1$. These two threshold conditions make it possible to sort the dynamic behavior of our system. In Section 3, we present our main theoretical findings on the stability of our dynamical system. In Section 4, we belay the exactitude of our outcomes by discussing the impact of non-integer orders on the stability behavior of system (2).

2 Well-posedness and definition of possible steady points

The first concern in analyzing the dynamical properties of a mathematical population system is to know whether it is well-posed or not, and we mean by well-posedness here that the system admits a unique, non-negative, and global-in-time solution. In this section, we will provide a suitable hypothetical framework under which the well-posedness of system (2) is guaranteed. Moreover, we will show that our model has three equilibrium points.

Existence, nonnegativity and boundedness of solutions

Before going the main result of this section, we first give the following useful lemma which will be involved in the sequel.

Lemma 1 *[36]. Assume that $\mathfrak{f}$ and ${}_0^{\mathcal{C}}\mathbb{F}^{\sigma}\mathfrak{f}$ are continuous functions on the interval $[\mathbf{a},\mathbf{b}]$, and $\sigma \in (0,1]$, then we have*

(i) If ${}_0^{\mathcal{C}}\mathbb{F}^{\sigma}\mathfrak{f}(t) \geq 0$ for all $t \in [\mathbf{a},\mathbf{b}]$, then $\mathfrak{f}$ is nondecreasing on $[\mathbf{a},\mathbf{b}]$,
(ii) If ${}_0^{\mathcal{C}}\mathbb{F}^{\sigma}\mathfrak{f}(t) \leq 0$ for all $t \in [\mathbf{a},\mathbf{b}]$, then $\mathfrak{f}$ is nonincreasing on $[\mathbf{a},\mathbf{b}]$.

Theorem 1 *The fractional model (2) with any nonnegative initial condition is well-posed in the sense that it has a unique nonnegative and bounded solution.*

Proof From Theorem 3.1 and Remark 3.2 in [37], we can prove the existence and uniqueness of the solution of system (2). Now, we show the nonnegativity of this solution. From system (2), one can deduce that

$${}_0^{\mathcal{C}}\mathbb{F}^{\sigma}\mathbf{U}\Big|_{\mathbf{U}=0} = \varphi + \xi\mathbf{X} > 0 \quad \text{for all } \mathbf{X},\mathbf{Y},\mathbf{W} \geq 0,$$

$${}_0^{\mathcal{C}}\mathbb{F}^{\sigma}\mathbf{X}\Big|_{\mathbf{X}=0} = \frac{\mathfrak{b}\mathbf{U}\mathbf{Y}}{1+q\mathbf{W}} \geq 0 \quad \text{for all } \mathbf{U},\mathbf{Y},\mathbf{W} \geq 0,$$

$${}_0^{\mathcal{C}}\mathbb{F}^{\sigma}\mathbf{Y}\Big|_{\mathbf{Y}=0} = k\mathbf{X} \geq 0 \quad \text{for all } \mathbf{U},\mathbf{X},\mathbf{W} \geq 0,$$

$${}_0^{\mathcal{C}}\mathbb{F}^{\sigma}\mathbf{W}\Big|_{\mathbf{W}=0} = 0 \geq 0 \quad \text{for all } \mathbf{U},\mathbf{X},\mathbf{Y} \geq 0.$$

By utilizing Lemma 1, we deduce that the solution of the fractional order system (2) is nonnegative. Now, we check the boundedness of the solution. For this purpose, we define the following function

$$\mathcal{N}(t) = \mathbf{U}(t) + \mathbf{X}(t) + \frac{\mathfrak{h}_2}{2k}\mathbf{Y}(t) + \frac{p\mathfrak{h}_2}{2kc}\mathbf{W}(t).$$

Thus,

$${}_0^{\mathcal{C}}\mathbb{F}^{\sigma}\mathcal{N}(t) = \varphi - \mathfrak{h}_1\mathbf{U}(t) - \frac{\mathfrak{h}_2}{2}\mathbf{X}(t) - \frac{\mathfrak{h}_2\mathfrak{h}_3}{2k}\mathbf{Y}(t) - \frac{p\mathfrak{h}_2\mathfrak{h}_4}{2kc}\mathbf{W}(t) \leq \varphi - d\mathcal{N}(t),$$

where $d = \min\left\{\hbar_1, \frac{\hbar_2}{2}, \hbar_3, \hbar_4\right\}$. Then, by Lemma 3 in [38], we obtain that

$$\mathcal{N}(t) \leq \left(\mathcal{N}(0) - \frac{\varphi}{d}\right)\mathcal{M}_\sigma\left(-dt^\sigma\right) + \frac{\varphi}{d},$$

where $\mathcal{M}_\sigma(z) = \sum_{j=0}^{\infty} \frac{z^j}{\Gamma(\sigma j+1)}$ is the Mittag-Leffler function of parameter σ [39]. Hence, $\limsup_{t\to\infty} \mathcal{N}(t) \leq \frac{\varphi}{d}$, Therefore, the solution of system (2) is bounded. ■

The steady states

Definition 1 *[40]. $\mathcal{O}^*$ is an equilibrium point of the system ${}_0^C\mathbb{F}^\sigma \mathfrak{f}(t) = \mathcal{P}(t, \mathfrak{f}(t))$, $\sigma \in (0,1]$, if $\mathcal{P}(t, \mathcal{O}^*) = 0$.*

The model (2) admits three biological steady points. Effortlessly, one can first deduce that the system (2) always has a virus-clear steady point

$$\mathbb{S}^\circ = (\mathbf{U}^\circ, 0, 0, 0) = \left(\frac{\varphi}{\hbar_1}, 0, 0, 0\right).$$

Then, we obtain the following basic reproduction number:

$$\mathcal{T}_\circ = \frac{\mathfrak{b}k\mathbf{U}^\circ}{\hbar_3(\hbar_2 + \xi)}.$$

Biologically, $\mathcal{T}_\circ$ indicates the mean density of the newly contaminated cells generated from one tainted cell at the beginning of the infection. If $\mathcal{T}_\circ > 1$, system (2) has the following immunity-free steady point:

$$\mathbb{S}_1^\star = (\mathbf{U}_1^\star, \mathbf{X}_1^\star, \mathbf{Y}_1^\star, 0) = \left(\frac{\hbar_3(\hbar_2 + \xi)}{\mathfrak{b}k}, \frac{\hbar_1\hbar_3(\hbar_2 + \xi)}{\mathfrak{b}\hbar_2 k}(\mathcal{T}_\circ - 1), \frac{k}{\hbar_3}\mathbf{X}_1^\star, 0\right).$$

Now, we set

$$\mathcal{T}_1 = \frac{c}{\hbar_4}\mathbf{Y}_1^\star = \frac{c\hbar_1(\hbar_2 + \xi)}{\mathfrak{b}\hbar_2\hbar_4}(\mathcal{T}_\circ - 1),$$

which is the immune response critical value. Explicitly, $\mathcal{T}_1$ refers to the average density of new immune cells provided by an immune cell over its natural mean lifespan [4]. If $\mathcal{T}_1 > 1$, system (2) has an immunity-activated steady point with humoral response $\mathbb{S}_2^\star = (\mathbf{U}_2^\star, \mathbf{X}_2^\star, \mathbf{Y}_2^\star, \mathbf{W}_2^\star)$, where

$$\begin{aligned}
\mathbf{U}_2^\star &= \frac{c\varphi(\hbar_2 + \xi)(1 + q\mathbf{W}_2^\star)}{\mathfrak{b}\hbar_2\hbar_4 + c\hbar_1(\hbar_2 + \xi)(1 + q\mathbf{W}_2^\star)},\\
\mathbf{X}_2^\star &= \frac{\mathfrak{b}\varphi\hbar_4}{\mathfrak{b}\hbar_2\hbar_4 + c\hbar_1(\hbar_2 + \xi)(1 + q\mathbf{W}_2^\star)},\\
\mathbf{Y}_2^\star &= \frac{\hbar_4}{c},
\end{aligned}$$

and $\mathbf{W}_2^\star$ is the positive real root of the following equation

$$\Omega_1\mathbf{W}_2^{\star 2} + \Omega_2\mathbf{W}_2^\star + \Omega_3 = 0,$$

where

$$\begin{aligned}
\Omega_1 &= cpq\hbar_1\hbar_4(\hbar_2 + \xi),\\
\Omega_2 &= \mathfrak{b}p\hbar_2\hbar_4^2 + c\hbar_1\hbar_4(\hbar_2 + \xi)(p + \hbar_3 q),\\
\Omega_3 &= \mathfrak{b}\hbar_2\hbar_3\hbar_4^2(1 - \mathcal{T}_1).
\end{aligned}$$

The results of this subsection can be summarized in the following theorem.

Theorem 2 *The fractional system (2) has three steady points. That is,*

i. if $\mathcal{T}_\circ \leq 1$, then model (2) has a unique virus-clear steady point $\mathbb{S}^\circ$,
ii. if $\mathcal{T}_1 \leq 1 < \mathcal{T}_\circ$, then model (2) has a unique immunity-free steady point $\mathbb{S}_1^\star$ besides $\mathbb{S}^\circ$,
iii. if $\mathcal{T}_1 > 1$, then model (2) has a unique immunity-activated steady point with humoral response $\mathbb{S}_2^\star$ besides $\mathbb{S}^\circ$ and $\mathbb{S}_1^\star$.

3 Stability characterization

This section is dedicated to examining the stability of $\mathbb{S}^\circ$, $\mathbb{S}_1^\star$ and $\mathbb{S}_2^\star$. To analyze the local stability of the equilibria, we need the following lemma.

Lemma 2 *[41]. Consider the fractional order system*

$$ {}_0^C\mathbb{F}^\sigma x(t) = h(x(t)), \;\; x(0) = x_0, $$

where $\sigma \in (0,1]$, $x(t) \in \mathbb{R}^n$ *and* $h \in C^1(\mathbb{R}^n, \mathbb{R}^n)$. *An equilibrium point is locally asymptotically stable if all the eigenvalues* η_j $(j = 1, 2, \ldots, n)$ *of the Jacobian matrix* $\mathbb{M}^{\mathcal{J}} = \frac{\partial h}{\partial x}$ *evaluated at the equilibrium satisfy* $\left|\arg(\eta_j)\right| > \frac{\sigma\pi}{2}$, *and unstable if there exist an eigenvalue* η_j *such that* $\left|\arg(\eta_j)\right| < \frac{\sigma\pi}{2}$.

It should be noted that the Jacobian matrix of (2) at any steady point $\mathbb{S} = (\mathbf{U}, \mathbf{X}, \mathbf{Y}, \mathbf{W})$ is given as follows:

$$ \mathbb{M}^{\mathcal{J}} = \begin{pmatrix} -\hbar_1 - \frac{\flat\mathbf{Y}}{1+q\mathbf{W}} & \xi & -\frac{\flat\mathbf{U}}{1+q\mathbf{W}} & \frac{\flat q\mathbf{U}\mathbf{Y}}{(1+q\mathbf{W})^2} \\ \frac{\flat\mathbf{Y}}{1+q\mathbf{W}} & -\hbar_2 - \xi & \frac{\flat\mathbf{U}}{1+q\mathbf{W}} & -\frac{\flat q\mathbf{U}\mathbf{Y}}{(1+q\mathbf{W})^2} \\ 0 & k & -\hbar_3 - p\mathbf{W} & -p\mathbf{Y} \\ 0 & 0 & c\mathbf{W} & -\hbar_4 + c\mathbf{Y} \end{pmatrix}. \tag{3} $$

In order to prove the global stability, we need the two following lemmas.

Lemma 3 *[42]. Let* $o(t) \in \mathbb{R}_+$ *be a continuous and differentiable function. Then, for any* $t \geq 0$, $\sigma \in (0,1]$, *and* $o^* > 0$, *we have*

$$ {}_0^C\mathbb{F}^\sigma \left(o(t) - o^* - o^* \ln \frac{o(t)}{o^*} \right) \leq \left(1 - \frac{o^*}{o(t)} \right) {}_0^C\mathbb{F}^\sigma o(t). $$

Lemma 4 *[43]. Let* $o(t) \in \mathbb{R}_+$ *be a continuous and differentiable function. Then, for any* $t \geq 0$ *and* $\sigma \in (0,1]$, *we have*

$$ \frac{1}{2} {}_0^C\mathbb{F}^\sigma o^2(t) \leq o(t) \, {}_0^C\mathbb{F}^\sigma o(t). $$

We will also need the following fractional version of the well-known LaSalle's invariance principle.

Lemma 5 *[44]. Suppose* $\mathcal{E}$ *is a bounded closed set. Every solution of system* ${}_0^C\mathbb{F}^\sigma x(t) = f(x(t))$ *starts from a point in* $\mathcal{E}$ *and remains in* $\mathcal{E}$ *for all time. If* $\exists\, \mathcal{L} \in C^1(\mathcal{E}, \mathbb{R})$ *such that* ${}_0^C\mathbb{F}^\sigma \mathcal{L}(x(t)) \leq 0$. *Let* $D = \left\{ x \in \mathcal{E} : {}_0^C\mathbb{F}^\sigma \mathcal{L} = 0 \right\}$ *and* $\mathcal{M}$ *be the largest invariant set of D. Then every solution* $x(t)$ *originating in* $\mathcal{E}$ *tends to* $\mathcal{M}$ *as* $t \to \infty$. *In particular, if* $\mathcal{M} = \{0\}$, $x(t) \to 0$ *as* $t \to \infty$.

Stability of the virus-clear steady point $\mathbb{S}^\circ$

Theorem 3 *If* $\mathcal{T}_\circ < 1$, *then* $\mathbb{S}^\circ$ *is locally asymptotically stable for all* $\sigma \in (0,1]$. $\mathbb{S}^\circ$ *is unstable if* $\mathcal{T}_\circ > 1$.

Proof The characteristic equation of the Jacobian matrix (3) at $\mathbb{S}^\circ$ is given by

$$ (\eta + \hbar_1)(\eta + \hbar_4) \left[\eta^2 + (\hbar_2 + \hbar_3 + \xi)\eta + \hbar_3(\hbar_2 + \xi) - \flat k\mathbf{U}^\circ \right] = 0. \tag{4} $$

Plainly, equation (4) has two negative real roots $\eta_1 = -\hbar_1$ and $\eta_2 = -\hbar_4$, then $\left|\arg(\eta_{1,2})\right| = \pi > \frac{\sigma\pi}{2}$ for any $\sigma \in (0,1]$. The other two roots of (4) are governed by the following equation:

$$ \eta^2 + (\hbar_2 + \hbar_3 + \xi)\eta + \hbar_3(\hbar_2 + \xi)(1 - \mathcal{T}_\circ) = 0, \tag{5} $$

which has, by the Routh-Hurwitz criterion, two roots η_i $(i = 3, 4)$ with negative real parts if $\mathcal{T}_\circ < 1$. Thus, $\left|\arg(\eta_{3,4})\right| > \frac{\pi}{2} \geq \frac{\sigma\pi}{2}$ for any $\sigma \in (0,1]$ when $\mathcal{T}_\circ < 1$. If $\mathcal{T}_\circ > 1$, then equation (5) admits a positive real root η^*, then $\left|\arg(\eta^*)\right| = 0 < \frac{\sigma\pi}{2}$ for all $\sigma \in (0,1]$. Consequently, by Lemma 2, $\mathbb{S}^\circ$ is unstable if $\mathcal{T}_\circ > 1$ and locally asymptotically stable if $\mathcal{T}_\circ < 1$. ■

Theorem 4 *If* $\mathcal{T}_\circ \leq 1$, *then* $\mathbb{S}^\circ$ *is globally asymptotically stable for all* $\sigma \in (0,1]$.

Proof Let $\mathcal{L}_{\star\star}$ be the Lyapunov functional defined as

$$ \mathcal{L}_{\star\star}(t) = \mathbf{U}^\circ H\left(\frac{\mathbf{U}(t)}{\mathbf{U}^\circ}\right) + \mathbf{X}(t) + \frac{\flat\mathbf{U}^\circ}{\hbar_3}\mathbf{Y}(t) + \frac{\flat p\mathbf{U}^\circ}{c\hbar_3}\mathbf{W}(t) + \frac{\xi}{2(\hbar_1 + \hbar_2)\mathbf{U}^\circ}\left(\mathbf{U}(t) - \mathbf{U}^\circ + \mathbf{X}(t)\right)^2, $$

where $H(x) = x - 1 - \ln x,\ x > 0$. According to Lemma 3 and Lemma 4, we obtain

$$\begin{aligned}
{}_0^{\mathcal{C}}\mathbb{F}^{\sigma}\mathcal{L}_{\star\star} &\leq \left(1 - \frac{\mathbf{U}^{\circ}}{\mathbf{U}}\right) {}_0^{\mathcal{C}}\mathbb{F}^{\sigma}\mathbf{U} + {}_0^{\mathcal{C}}\mathbb{F}^{\sigma}\mathbf{X} + \frac{\mathfrak{b}\mathbf{U}^{\circ}}{\mathfrak{h}_3}\, {}_0^{\mathcal{C}}\mathbb{F}^{\sigma}\mathbf{Y} + \frac{\mathfrak{b}p\mathbf{U}^{\circ}}{c\mathfrak{h}_3}\, {}_0^{\mathcal{C}}\mathbb{F}^{\sigma}\mathbf{W} \\
&\quad + \frac{\xi}{(\mathfrak{h}_1 + \mathfrak{h}_2)\mathbf{U}^{\circ}} (\mathbf{U} - \mathbf{U}^{\circ} + \mathbf{X}) \left({}_0^{\mathcal{C}}\mathbb{F}^{\sigma}\mathbf{U} + {}_0^{\mathcal{C}}\mathbb{F}^{\sigma}\mathbf{X}\right) \\
&= \left(1 - \frac{\mathbf{U}^{\circ}}{\mathbf{U}}\right) \left(\varphi - \mathfrak{h}_1\mathbf{U} - \frac{\mathfrak{b}\mathbf{U}\mathbf{Y}}{1 + q\mathbf{W}} + \xi\mathbf{X}\right) + \frac{\mathfrak{b}\mathbf{U}\mathbf{Y}}{1 + q\mathbf{W}} - (\mathfrak{h}_2 + \xi)\mathbf{X} \\
&\quad + \frac{\mathfrak{b}\mathbf{U}^{\circ}}{\mathfrak{h}_3} (k\mathbf{X} - \mathfrak{h}_3\mathbf{Y} - p\mathbf{Y}\mathbf{W}) + \frac{\mathfrak{b}p\mathbf{U}^{\circ}}{c\mathfrak{h}_3} (c\mathbf{Y}\mathbf{W} - \mathfrak{h}_4\mathbf{W}) + \frac{\xi}{(\mathfrak{h}_1 + \mathfrak{h}_2)\mathbf{U}^{\circ}} (\mathbf{U} - \mathbf{U}^{\circ} + \mathbf{X}) (\varphi - \mathfrak{h}_1\mathbf{U} - \mathfrak{h}_2\mathbf{X}) \\
&= -\mathfrak{h}_1 \frac{(\mathbf{U} - \mathbf{U}^{\circ})^2}{\mathbf{U}} + \xi\mathbf{X}\left(1 - \frac{\mathbf{U}^{\circ}}{\mathbf{U}}\right) + \frac{\mathfrak{b}\mathbf{U}^{\circ}\mathbf{Y}}{1 + q\mathbf{W}} - (\mathfrak{h}_2 + \xi)\mathbf{X} - \mathfrak{b}\mathbf{U}^{\circ}\mathbf{Y} + \frac{\mathfrak{b}k\mathbf{U}^{\circ}}{\mathfrak{h}_3}\mathbf{X} - \frac{\mathfrak{b}p\mathfrak{h}_4\mathbf{U}^{\circ}}{c\mathfrak{h}_3}\mathbf{W} \\
&\quad - \frac{\xi}{(\mathfrak{h}_1 + \mathfrak{h}_2)\mathbf{U}^{\circ}} (\mathbf{U} - \mathbf{U}^{\circ} + \mathbf{X}) (\mathfrak{h}_1 (\mathbf{U} - \mathbf{U}^{\circ}) + \mathfrak{h}_2\mathbf{X}) \\
&= -\left(\mathfrak{h}_1\mathbf{U}^{\circ} + \xi\mathbf{X} + \frac{\xi\mathfrak{h}_1\mathbf{U}}{\mathfrak{h}_1 + \mathfrak{h}_2}\right) \frac{(\mathbf{U} - \mathbf{U}^{\circ})^2}{\mathbf{U}\mathbf{U}^{\circ}} - \frac{\mathfrak{h}_2\xi\mathbf{X}^2}{(\mathfrak{h}_1 + \mathfrak{h}_2)\mathbf{U}^{\circ}} - \frac{\mathfrak{b}q\mathbf{U}^{\circ}\mathbf{Y}\mathbf{W}}{1 + q\mathbf{W}} - \frac{\mathfrak{b}p\mathfrak{h}_4\mathbf{U}^{\circ}\mathbf{W}}{c\mathfrak{h}_3} + (\mathfrak{h}_2 + \xi)(\mathcal{T}_{\circ} - 1)\mathbf{X}.
\end{aligned}$$

Therefore, $\mathcal{T}_{\circ} \leq 1$ ensures that ${}_0^{\mathcal{C}}\mathbb{F}^{\sigma}\mathcal{L}_{\star\star} \leq 0$. Furthermore, it is easy to verify that the singleton $\{\mathbb{S}^{\circ}\}$ is the largest compact invariant set in $\left\{(\mathbf{U}, \mathbf{X}, \mathbf{Y}, \mathbf{W}) \in \mathbb{R}_+^4 : {}_0^{\mathcal{C}}\mathbb{F}^{\sigma}\mathcal{L}_{\star\star} = 0\right\}$. By Lemma 5, we infer that $\mathbb{S}^{\circ}$ is globally asymptotically stable if $\mathcal{T}_{\circ} \leq 1$ for all $\sigma \in (0, 1]$. ■

Stability of the immune-free steady point $\mathbb{S}_1^{\star}$

This subsection aims to analyze the stability of the immune-free steady point $\mathbb{S}_1^{\star}$ of the system (2). Obviously, we presume that $\mathcal{T}_{\circ} > 1$.

Theorem 5 *If $\mathcal{T}_1 < 1 < \mathcal{T}_{\circ}$, then $\mathbb{S}_1^{\star}$ is locally asymptotically stable for all $\sigma \in (0, 1]$. $\mathbb{S}_1^{\star}$ is unstable if $\mathcal{T}_1 > 1$.*

Proof At $\mathbb{S}_1^{\star}$, the characteristic equation of the Jacobian matrix (3) is given by

$$(\eta + \mathfrak{h}_4 - c\mathbf{Y}_1^{\star}) \left(\eta^3 + \Pi_2\eta^2 + \Pi_1\eta + \Pi_0\right) = 0, \tag{6}$$

where

$$\begin{aligned}
\Pi_2 &= \mathfrak{h}_1 + \mathfrak{h}_2 + \mathfrak{h}_3 + \xi + \mathfrak{b}\mathbf{Y}_1^{\star}, \\
\Pi_1 &= \mathfrak{h}_1 (\mathfrak{h}_2 + \mathfrak{h}_3 + \xi) + \mathfrak{b}\mathbf{Y}_1^{\star} (\mathfrak{h}_2 + \mathfrak{h}_3), \\
\Pi_0 &= \mathfrak{h}_2\mathfrak{h}_3\mathfrak{b}\mathbf{Y}_1^{\star}.
\end{aligned}$$

One of the roots of equation (6) is $\eta_1 = c\mathbf{Y}_1^{\star} - \mathfrak{h}_4 = \mathfrak{h}_4(\mathcal{T}_1 - 1)$. Hence, $|\arg(\eta_1)| = \pi > \frac{\sigma\pi}{2}$ for all $\sigma \in (0, 1]$ if $\mathcal{T}_1 < 1$ and $|\arg(\eta_1)| = 0 < \frac{\sigma\pi}{2}$ for all $\sigma \in (0, 1]$ if $\mathcal{T}_1 > 1$. While the remaining roots are given by the solution to the following equation:

$$\eta^3 + \Pi_2\eta^2 + \Pi_1\eta + \Pi_0 = 0. \tag{7}$$

It is easy to remark that $\Pi_2 > 0$, $\Pi_1 > 0$ and $\Pi_0 > 0$. Therefore,

$$\Pi_2\Pi_1 - \Pi_0 = (\mathfrak{h}_1 + \mathfrak{h}_2 + \xi + \mathfrak{b}\mathbf{Y}_1^{\star})\,\Pi_1 + \mathfrak{h}_1\mathfrak{h}_3\,(\mathfrak{h}_2 + \mathfrak{h}_3 + \xi) + \mathfrak{h}_3^2\mathfrak{b}\mathbf{Y}_1^{\star} > 0.$$

Thus, by the Routh-Hurwitz criterion, all roots η_i $(i = 2, 3, 4)$ of (7) have negative real part, so that $|\arg(\eta_{2,3,4})| > \frac{\pi}{2} \geq \frac{\sigma\pi}{2}$ for all $\sigma \in (0, 1]$ if $\mathcal{T}_{\circ} > 1$. In accordance with Lemma 1, $\mathbb{S}_1^{\star}$ is unstable if $\mathcal{T}_1 > 1$ and locally asymptotically stable if $\mathcal{T}_1 < 1 < \mathcal{T}_{\circ}$. ■

Next, we analyze the global stability of $\mathbb{S}_1^{\star}$ by assuming the following hypothesis

$$\frac{\mathbf{Y}_1^{\star}}{\mathbf{Y}} - \frac{1}{1 + q\mathbf{W}} \leq 0. \tag{$\mathcal{H}$}$$

Theorem 6 *If $\mathcal{T}_1 \leq 1 < \mathcal{T}_{\circ} \leq 1 + \frac{\mathfrak{h}_2}{\xi}$ and $(\mathcal{H})$ holds, then $\mathbb{S}_1^{\star}$ is globally asymptotically stable for any $\sigma \in (0, 1]$.*

Proof Let $\mathcal{L}_{\dagger}$ be the Lyapunov functional defined as

$$\begin{aligned}
\mathcal{L}_{\dagger}(t) &= \mathbf{U}_1^{\star} H\left(\frac{\mathbf{U}(t)}{\mathbf{U}_1^{\star}}\right) + \mathbf{X}_1^{\star} H\left(\frac{\mathbf{X}(t)}{\mathbf{X}_1^{\star}}\right) + \frac{\mathfrak{b}\mathbf{U}_1^{\star}\mathbf{Y}_1^{\star}}{k\mathbf{X}_1^{\star}}\mathbf{Y}_1^{\star} H\left(\frac{\mathbf{Y}(t)}{\mathbf{Y}_1^{\star}}\right) + \frac{\mathfrak{b}p\mathbf{U}_1^{\star}\mathbf{Y}_1^{\star}}{ck\mathbf{X}_1^{\star}}\mathbf{W}(t) \\
&\quad + \frac{\xi}{2(\mathfrak{h}_1 + \mathfrak{h}_2)\mathbf{U}_1^{\star}} (\mathbf{U}(t) - \mathbf{U}_1^{\star} + \mathbf{X}(t) - \mathbf{X}_1^{\star})^2.
\end{aligned}$$

Applying the Caputo fractional derivative on system (2), we obtain

$$\begin{aligned}
{}_0^{\mathcal{C}}\mathbb{F}^{\sigma}\mathcal{L}_{\dagger} \leq{}& \left(1-\frac{\mathbf{U}_1^{\star}}{\mathbf{U}}\right){}_0^{\mathcal{C}}\mathbb{F}^{\sigma}\mathbf{U}+\left(1-\frac{\mathbf{X}_1^{\star}}{\mathbf{X}}\right){}_0^{\mathcal{C}}\mathbb{F}^{\sigma}\mathbf{X}+\frac{\mathfrak{b}\mathbf{U}_1^{\star}\mathbf{Y}_1^{\star}}{k\mathbf{X}_1^{\star}}\left(1-\frac{\mathbf{Y}_1^{\star}}{\mathbf{Y}}\right){}_0^{\mathcal{C}}\mathbb{F}^{\sigma}\mathbf{Y}+\frac{\mathfrak{b}p\mathbf{U}_1^{\star}\mathbf{Y}_1^{\star}}{ck\mathbf{X}_1^{\star}}{}_0^{\mathcal{C}}\mathbb{F}^{\sigma}\mathbf{W}\\
&+\frac{\xi}{(\mathfrak{h}_1+\mathfrak{h}_2)\mathbf{U}_1^{\star}}(\mathbf{U}-\mathbf{U}_1^{\star}+\mathbf{X}-\mathbf{X}_1^{\star})\left({}_0^{\mathcal{C}}\mathbb{F}^{\sigma}\mathbf{U}+{}_0^{\mathcal{C}}\mathbb{F}^{\sigma}\mathbf{X}\right)\\
={}&\left(1-\frac{\mathbf{U}_1^{\star}}{\mathbf{U}}\right)\left(\varphi-\mathfrak{h}_1\mathbf{U}-\frac{\mathfrak{b}\mathbf{U}\mathbf{Y}}{1+q\mathbf{W}}+\xi\mathbf{X}\right)+\left(1-\frac{\mathbf{X}_1^{\star}}{\mathbf{X}}\right)\left(\frac{\mathfrak{b}\mathbf{U}\mathbf{Y}}{1+q\mathbf{W}}-(\mathfrak{h}_2+\xi)\mathbf{X}\right)\\
&+\frac{\mathfrak{b}\mathbf{U}_1^{\star}\mathbf{Y}_1^{\star}}{k\mathbf{X}_1^{\star}}\left(1-\frac{\mathbf{Y}_1^{\star}}{\mathbf{Y}}\right)(k\mathbf{X}-\mathfrak{h}_3\mathbf{Y}-p\mathbf{Y}\mathbf{W})+\frac{\mathfrak{b}p\mathbf{U}_1^{\star}\mathbf{Y}_1^{\star}}{ck\mathbf{X}_1^{\star}}(c\mathbf{Y}\mathbf{W}-\mathfrak{h}_4\mathbf{W})\\
&+\frac{\xi}{(\mathfrak{h}_1+\mathfrak{h}_2)\mathbf{U}_1^{\star}}(\mathbf{U}-\mathbf{U}_1^{\star}+\mathbf{X}-\mathbf{X}_1^{\star})(\varphi-\mathfrak{h}_1\mathbf{U}-\mathfrak{h}_2\mathbf{X}).
\end{aligned}$$

Note that $\varphi=\mathfrak{h}_1\mathbf{U}_1^{\star}+\mathfrak{b}\mathbf{U}_1^{\star}\mathbf{Y}_1^{\star}-\xi\mathbf{X}_1^{\star}$, $\mathfrak{h}_2+\xi=\frac{\mathfrak{b}\mathbf{U}_1^{\star}\mathbf{Y}_1^{\star}}{\mathbf{X}_1^{\star}}$ and $\mathfrak{h}_3=\frac{k\mathbf{X}_1^{\star}}{\mathbf{Y}_1^{\star}}$. Therefore,

$$\begin{aligned}
{}_0^{\mathcal{C}}\mathbb{F}^{\sigma}\mathcal{L}_{\dagger} \leq{}& \mathfrak{h}_1\left(1-\frac{\mathbf{U}_1^{\star}}{\mathbf{U}}\right)(\mathbf{U}_1^{\star}-\mathbf{U})+\xi(\mathbf{X}-\mathbf{X}_1^{\star})\left(1-\frac{\mathbf{U}_1^{\star}}{\mathbf{U}}\right)\\
&+\mathfrak{b}\mathbf{U}_1^{\star}\mathbf{Y}_1^{\star}\left(3-\frac{\mathbf{U}_1^{\star}}{\mathbf{U}}+\frac{\mathbf{Y}}{\mathbf{Y}_1^{\star}}\frac{1}{1+q\mathbf{W}}-\frac{\mathbf{U}\mathbf{X}_1^{\star}\mathbf{Y}}{\mathbf{U}_1^{\star}\mathbf{X}\mathbf{Y}_1^{\star}}\frac{1}{1+q\mathbf{W}}-\frac{\mathbf{Y}}{\mathbf{Y}_1^{\star}}-\frac{\mathbf{X}\mathbf{Y}_1^{\star}}{\mathbf{X}_1^{\star}\mathbf{Y}}\right)\\
&+\frac{\mathfrak{b}p\mathbf{U}_1^{\star}\mathbf{Y}_1^{\star}}{k\mathbf{X}_1^{\star}}\left(\mathbf{Y}_1^{\star}-\frac{\mathfrak{h}_4}{c}\right)\mathbf{W}-\frac{\xi}{(\mathfrak{h}_1+\mathfrak{h}_2)\mathbf{U}_1^{\star}}(\mathbf{U}-\mathbf{U}_1^{\star}+\mathbf{X}-\mathbf{X}_1^{\star})(\mathfrak{h}_1(\mathbf{U}-\mathbf{U}_1^{\star})+\mathfrak{h}_2(\mathbf{X}-\mathbf{X}_1^{\star}))\\
={}&-\left(\mathfrak{h}_1\mathbf{U}_1^{\star}+\xi\mathbf{X}-\xi\mathbf{X}_1^{\star}+\frac{\xi\mathfrak{h}_1\mathbf{U}}{\mathfrak{h}_1+\mathfrak{h}_2}\right)\frac{(\mathbf{U}-\mathbf{U}_1^{\star})^2}{\mathbf{U}\mathbf{U}_1^{\star}}-\frac{\xi\mathfrak{h}_2}{(\mathfrak{h}_1+\mathfrak{h}_2)\mathbf{U}_1^{\star}}(\mathbf{X}-\mathbf{X}_1^{\star})^2\\
&+\mathfrak{b}\mathbf{U}_1^{\star}\mathbf{Y}_1^{\star}\left(4-\frac{\mathbf{U}_1^{\star}}{\mathbf{U}}-(1+q\mathbf{W})-\frac{\mathbf{U}\mathbf{X}_1^{\star}\mathbf{Y}}{\mathbf{U}_1^{\star}\mathbf{X}\mathbf{Y}_1^{\star}}\frac{1}{1+q\mathbf{W}}-\frac{\mathbf{X}\mathbf{Y}_1^{\star}}{\mathbf{X}_1^{\star}\mathbf{Y}}\right)\\
&+\mathfrak{b}q\mathbf{U}_1^{\star}\mathbf{Y}_1^{\star}\left(1-\frac{\mathbf{Y}}{\mathbf{Y}_1^{\star}}\frac{1}{1+q\mathbf{W}}\right)\mathbf{W}+\frac{\mathfrak{h}_4\mathfrak{b}p\mathbf{U}_1^{\star}\mathbf{Y}_1^{\star}}{ck\mathbf{X}_1^{\star}}(\mathcal{T}_1-1)\mathbf{W}.
\end{aligned}$$

Employing the arithmetic-geometric means inequality, we obtain

$$4-\frac{\mathbf{U}_1^{\star}}{\mathbf{U}}-(1+q\mathbf{W})-\frac{\mathbf{U}\mathbf{X}_1^{\star}\mathbf{Y}}{\mathbf{U}_1^{\star}\mathbf{X}\mathbf{Y}_1^{\star}}\frac{1}{1+q\mathbf{W}}-\frac{\mathbf{X}\mathbf{Y}_1^{\star}}{\mathbf{X}_1^{\star}\mathbf{Y}}\leq 0.$$

From $(\mathcal{H})$, we have

$$1-\frac{\mathbf{Y}}{\mathbf{Y}_1^{\star}}\frac{1}{1+q\mathbf{W}}=\frac{\mathbf{Y}}{\mathbf{Y}_1^{\star}}\left(\frac{\mathbf{Y}_1^{\star}}{\mathbf{Y}}-\frac{1}{1+q\mathbf{W}}\right)\leq 0.$$

Further, we have

$$\mathfrak{h}_1\mathbf{U}_1^{\star}-\xi\mathbf{X}_1^{\star}=\frac{\mathfrak{h}_1\mathfrak{h}_3(\mathfrak{h}_2+\xi)}{\mathfrak{b}k}\left(1-\frac{\xi}{\mathfrak{h}_2}(\mathcal{T}_{\circ}-1)\right).$$

Thus, ${}_0^{\mathcal{C}}\mathbb{F}^{\sigma}\mathcal{L}_{\dagger}\leq 0$ if $\mathcal{T}_1\leq 1<\mathcal{T}_{\circ}\leq 1+\frac{\mathfrak{h}_2}{\xi}$. Furthermore, the largest compact invariant set in $\left\{(\mathbf{U},\mathbf{X},\mathbf{Y},\mathbf{W})\in\mathbb{R}_+^4:\ {}_0^{\mathcal{C}}\mathbb{F}^{\sigma}\mathcal{L}_{\dagger}=0\right\}$ is singleton $\{\mathbb{S}_1^{\star}\}$. By Lemma 5, $\mathbb{S}_1^{\star}$ is globally asymptotically stable if $\mathcal{T}_1\leq 1<\mathcal{T}_{\circ}\leq 1+\frac{\mathfrak{h}_2}{\xi}$. ■

Stability of immunity-activated steady point with humoral response $\mathbb{S}_2^{\star}$

In this subsection, we deal with the local stability of the steady point $\mathbb{S}_2^{\star}$. We begin our analysis by computing the characteristic equation of the Jacobian matrix (3) at $\mathbb{S}_2^{\star}$, we find

$$\eta^4+\mathcal{O}_3\eta^3+\mathcal{O}_2\eta^2+\mathcal{O}_1\eta+\mathcal{O}_0=0, \tag{8}$$

where

$$\begin{aligned}
\mathcal{O}_3 &= \mathfrak{h}_1+\mathfrak{h}_2+\mathfrak{h}_3+\xi+p\mathbf{W}_2^{\star}+\frac{\mathfrak{b}\mathbf{Y}_2^{\star}}{1+q\mathbf{W}_2^{\star}}>0,\\
\mathcal{O}_2 &= \mathfrak{h}_4p\mathbf{W}_2^{\star}+\mathfrak{h}_1(\mathfrak{h}_2+\mathfrak{h}_3+\xi+p\mathbf{W}_2^{\star})+\frac{\mathfrak{b}\mathbf{Y}_2^{\star}}{1+q\mathbf{W}_2^{\star}}(\mathfrak{h}_2+\mathfrak{h}_3+p\mathbf{W}_2^{\star})>0,\\
\mathcal{O}_1 &= \mathfrak{h}_4p\mathbf{W}_2^{\star}(\mathfrak{h}_1+\mathfrak{h}_2+\xi)+\frac{\mathfrak{b}\mathbf{Y}_2^{\star}}{1+q\mathbf{W}_2^{\star}}(\mathfrak{h}_4p\mathbf{W}_2^{\star}+\mathfrak{h}_2(\mathfrak{h}_3+p\mathbf{W}_2^{\star}))+\frac{kcq\mathfrak{b}\mathbf{U}_2^{\star}\mathbf{Y}_2^{\star}\mathbf{W}_2^{\star}}{(1+q\mathbf{W}_2^{\star})^2}>0,\\
\mathcal{O}_0 &= \mathfrak{h}_1\mathfrak{h}_4p\mathbf{W}_2^{\star}(\mathfrak{h}_2+\xi)+\mathfrak{h}_2\mathfrak{h}_4p\mathbf{W}_2^{\star}\frac{\mathfrak{b}\mathbf{Y}_2^{\star}}{1+q\mathbf{W}_2^{\star}}+\mathfrak{h}_1kc\frac{\mathfrak{b}q\mathbf{U}_2^{\star}\mathbf{Y}_2^{\star}\mathbf{W}_2^{\star}}{(1+q\mathbf{W}_2^{\star})^2}>0.
\end{aligned}$$

Thus, by the Routh-Hurwitz criterion, all roots η_j ($j = 1, 2, 3, 4$) of (8) have negative real part if

$$\mathcal{O}_3\mathcal{O}_2 - \mathcal{O}_1 > 0 \text{ and } \mathcal{O}_1(\mathcal{O}_3\mathcal{O}_2 - \mathcal{O}_1) - \mathcal{O}_3^2\mathcal{O}_0 > 0, \tag{9}$$

so that $\left|\arg(\eta_j)\right| > \frac{\pi}{2} \geq \frac{\sigma\pi}{2}$ for all $\sigma \in (0, 1]$ if $\mathcal{T}_1 > 1$. Hence, according to Lemma 1, we have the following theorem.

Theorem 7 *Assume that $\mathcal{T}_1 > 1$ and the condition (9) holds, then $\mathbb{S}_2^\star$ is locally asymptotically stable for all $\sigma \in (0, 1]$.*

Remark 1 *Theorems 3, 4, 5, 6 and 7 indicate theoretically that the Caputo derivatives have no influence on the stability of the equilibria $\mathbb{S}^\circ$, $\mathbb{S}_1^\star$ and $\mathbb{S}_2^\star$.*

4 Numerical results and discussions

In this section, and by utilizing the parameter values of the data listed in Table 1, we discuss the different results established previously in this article. The pivotal purpose is to examine the influence of fractional derivatives on the long-run behavior of our enhanced model (2). We will theoretically choose the parameters used in the simulations according to two criteria:
1. To verify and check appropriately the obtained analytical results in all cases.
2. To show numerically the sharpness of the obtained stability conditions. During the forthcoming numerical tests, the solution of our viral system (2) is supposed to be starting from the initial condition $\mathbf{U}(0) = 300$, $\mathbf{X}(0) = 7$, $\mathbf{Y}(0) = 4$, $\mathbf{W}(0) = 80$. Also, we deem from now on that the unity of time is one day.

Parameter	*Example 1*	*Example 2*	*Example 3*	*Source*
φ	2	2	6	Assumed
$\hbar_1$	0.01	0.01	0.01	[4]
$\mathfrak{b}$	0.01	0.02	0.02	[4]
q	0.5	0.5	0.5	[4]
ξ	0.01	0.01	0.01	[4]
$\hbar_2$	1.001	1.001	1.001	Assumed
$\hbar_3$	2.0003	2.0003	2.0003	Assumed
$\hbar_4$	0.3	0.3	0.3	[4]
k	0.9	2.9	2.9	Assumed
p	0.006	0.006	0.006	Assumed
c	0.1	0.1	0.1	[4]

Table 1. Some numerical values of the deterministic parameters used in the simulations

Remark 2 *In this section, we aim to numerically examine the impact of fractional derivatives on the long-term characteristics of the virus. For this reason, we simulate its progression using the parameters listed in Table 1. We mention that the parameters φ, $\mathfrak{b}$ and k are very sensitive and a slight variation in their values results in a significant dynamical bifurcation. Thus, we present some simulated scenarios in order to cover all cases of equilibrium stability.*

Example 1: Virus-clear steady point $\mathbb{S}^\circ$

To numerically probe the effect of fractional derivatives on the infection stability, we firstly assign to our system parameters the numerical values appearing in Table 1 - Example 1. A simple calculation gives $\mathcal{T}_\circ = 0.8911$ which is strictly less than one. From Theorem 2, there exists a virus-clear steady point $\mathbb{S}^\circ = (200, 0, 0, 0)$ of system (2). By choosing some arbitrary values of σ: 0.98; 0.94; 0.9; 0.88; 0.84; 0.8; 0.78; 0.76, we present the long-run behavior of the solutions in Figure 2. Specifically, in the case of $\sigma = 0.98$, we remark that the density of susceptible cells $\mathbf{U}$, after an initial slope, progressively rises and reaches the steady value $\frac{\varphi}{\hbar_1} = 200$. After a significant decrease followed by a gradual increase, the densities of $\mathbf{X}(t)$ and $\mathbf{Y}(t)$ return to decrease and end up being disappeared over time, while the density of $\mathbf{W}(t)$ decreases and converges to zero.
Now, by decreasing the value of σ to 0.94, we show that the solution suddenly changes its behavior shape, but finally converges to $\mathbb{S}^\circ$. To further exhibit this phenomenon, we choose various values between $\sigma = 0.94$ and $\sigma = 0.76$. We conclude that as the value of σ decreases, the solution slowly reaches the equilibrium $\mathbb{S}^\circ$. That is, the rate of convergence increases as the integer-order σ is closer to one. But, in all cases, solutions with different differentiation values reach the virus-clear state which actually confirms the result of Theorem 3. Consequently, the infection will be eradicated from the host body.

Example 2: Immune-free steady point $\mathbb{S}_1^\star$

In this example, we select the parameter values from Table 1 - Example 2. Then, we obtain $\mathcal{T}_\circ = 5.7426 > 1$ and $\mathcal{T}_1 = 0.7983 < 1$. In accordance with Theorem 2, the immune-free steady point $\mathbb{S}_1^\star$ exists since $\mathcal{T}_1 < 1 < \mathcal{T}_\circ$. To depict the effect of fractional derivatives on $\mathbb{S}_1^\star$, we arbitrarily select certain values of $\sigma = 0.98; 0.94; 0.9; 0.88; 0.84; 0.8; 0.78; 0.76$. In Figure 3, we see that after some pseudo periodic fluctuations, the densities of $\mathbf{U}(t)$, $\mathbf{X}(t)$ and $\mathbf{Y}(t)$ reach the stable level $\mathbf{U}_1^\star = 34.8276$, $\mathbf{X}_1^\star = 1.6517$ and $\mathbf{Y}_1^\star = 2.3950$, while the density of $\mathbf{W}(t)$ ultimately extinct. Since $\mathcal{T}_1 < 1 < \mathcal{T}_\circ$, the numerical outcome of this example confirms the stability result of Theorem 5. Hence, the infection becomes chronic one in the absence of persistent humoral immune response.

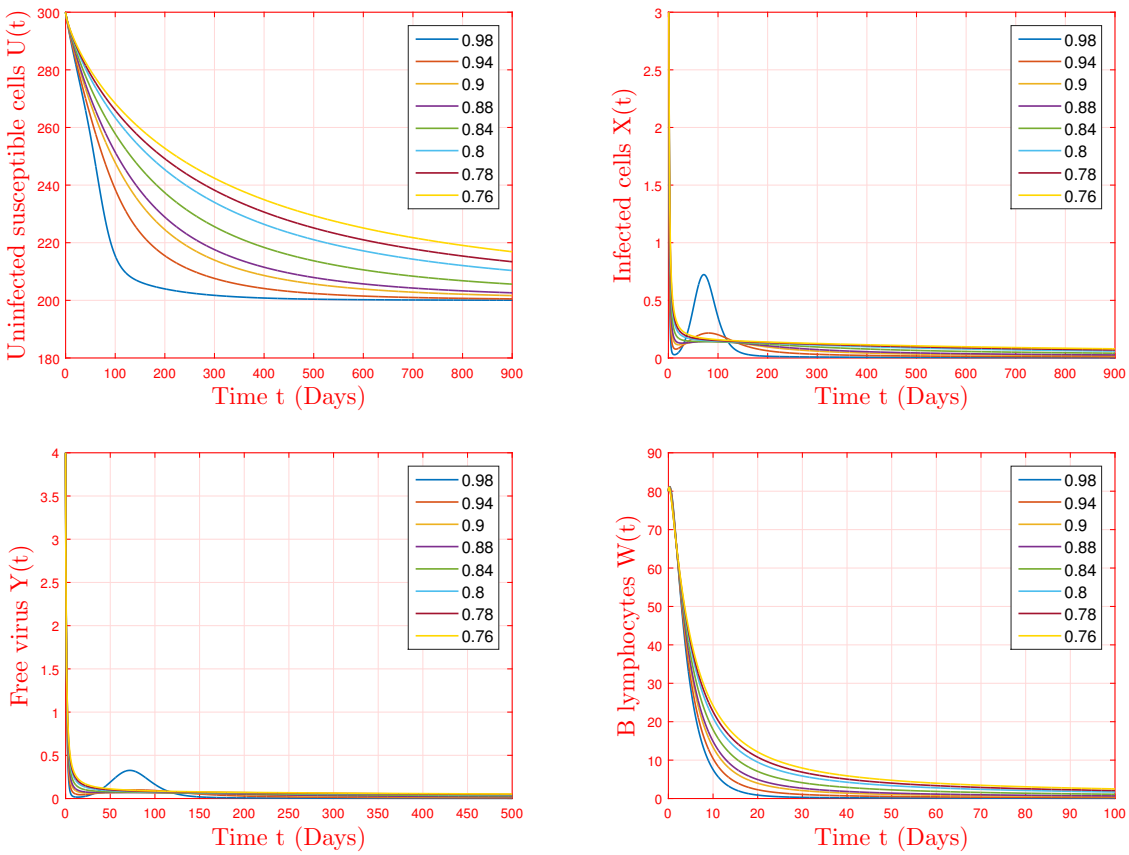

Figure 2. *Stability of the virus-clear steady point* $\mathbb{S}^{\circ} = (200, 0, 0, 0)$ *for different values of* $\sigma = 0.98; 0.94; 0.9; 0.88; 0.84; 0.8; 0.78; 0.76$.

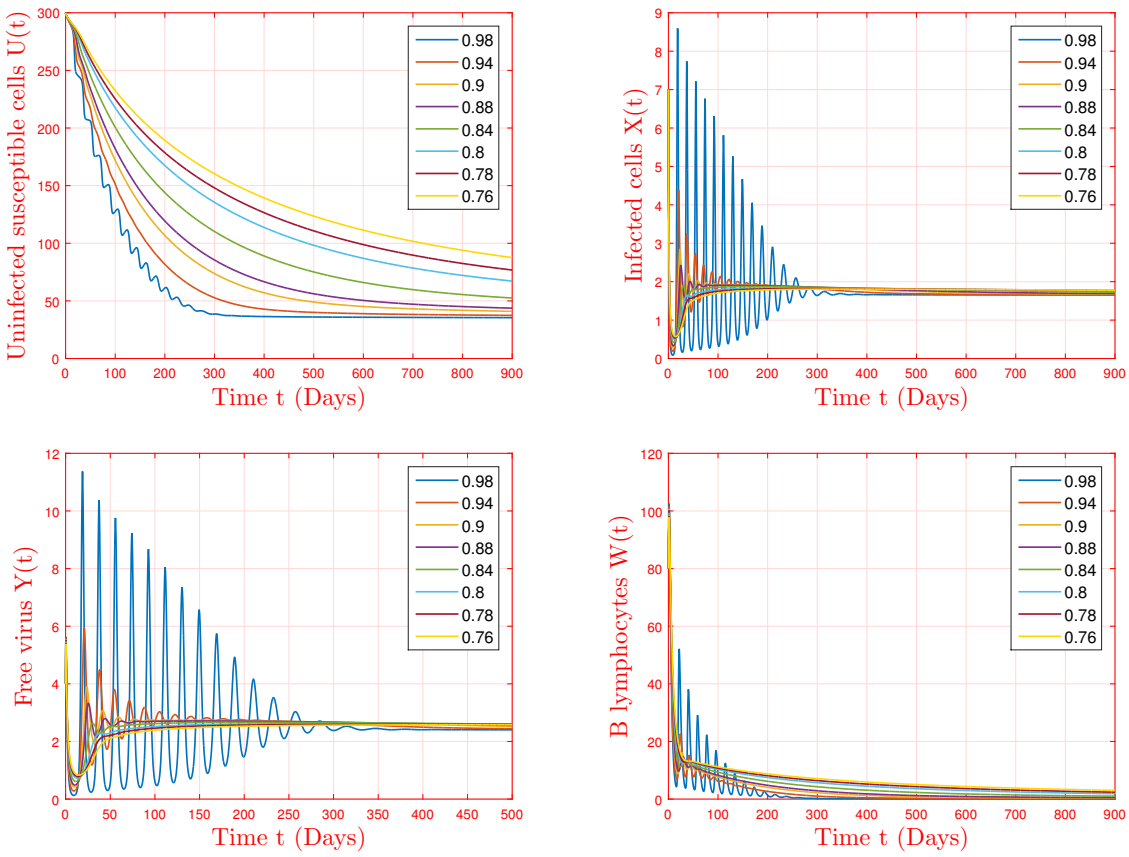

Figure 3. *Stability of the immune-free steady point* $\mathbb{S}_1^{\star} = (34.8276, 1.6517, 2.3950, 0)$ *for different values of* $\sigma = 0.98; 0.94; 0.9; 0.88; 0.84; 0.8; 0.78; 0.76$.

Example 3: Immunity-activated steady point with the humoral response $\mathbb{S}_2^\star$

Now, we choose the parameter values from Table 1 - Example 3. Then, we obtain $\mathcal{T}_1 = 2.7317 > 1$. In accordance with Theorem 2, there is an immunity-activated steady point with the humoral response $\mathbb{S}_2^\star$. Furthermore, we get

$$\mathcal{O}_3\mathcal{O}_2 - \mathcal{O}_1 = 0.3648 > 0,$$
$$\mathcal{O}_1\left(\mathcal{O}_3\mathcal{O}_2 - \mathcal{O}_1\right) - \mathcal{O}_3^2\mathcal{O}_0 = 0.2903 > 0,$$

then $\mathbb{S}_2^\star$ is asymptotically stable for different values of σ due to Theorem 7. From Figure 4, we remark that all classes fluctuate during a time phase then converge towards the steady values $\mathbf{U}_2^\star = 381.4716$, $\mathbf{X}_2^\star = 2.1853$, $\mathbf{Y}_2^\star = 3.0000$ and $\mathbf{W}_2^\star = 18.7403$. By selecting certain values of σ, we observe that the solutions always reach the steady point $\mathbb{S}_2^\star = (\mathbf{U}_2^\star, \mathbf{X}_2^\star, \mathbf{Y}_2^\star, \mathbf{W}_2^\star)$. Thus, the viral infection becomes chronic with persistent humoral immune response.

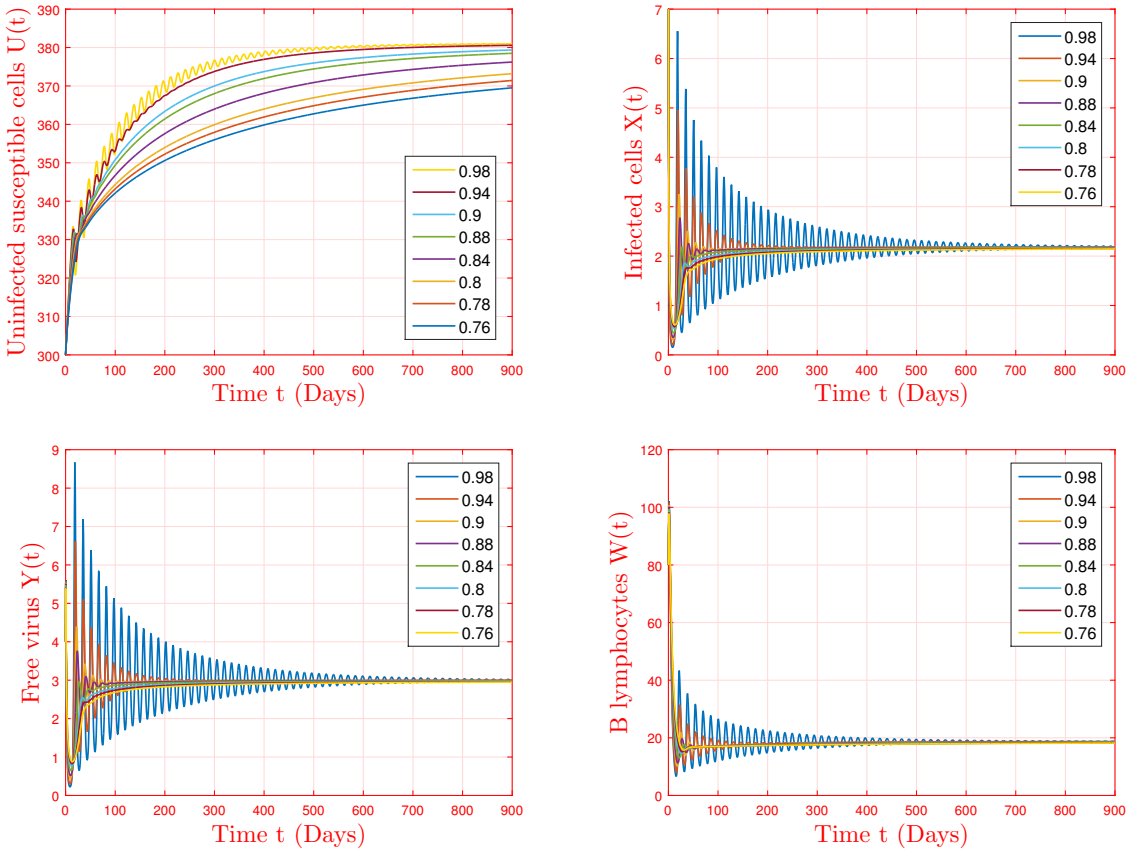

Figure 4. *Stability of the immunity-activated steady point with the humoral response* $\mathbb{S}_2^\star = (381.4716, 2.1853, 3.0000, 18.7403)$ *for different values of* $\sigma = 0.98; 0.94; 0.9; 0.88; 0.84; 0.8; 0.78; 0.76$.

5 Conclusion

This article investigated an improved four-compartment viral system that takes into consideration the effects of fractional derivatives. The central goal was to probe the long-term characteristics of the virus. For this reason, we have started by proved the well-posedness of the model, including existence, uniqueness, nonnegativity and boundedness of solutions. We have defined the steady points of the system and determining the associated critical thresholds, namely the basic reproduction number, $\mathcal{T}_\circ$, and the humoral immune response reproduction number, $\mathcal{T}_1$. Specifically, we have proved that our viral model admits three steady points, and under certain conditions on the thresholds, the asymptotic stability of all these points was examined. The obtained results of stability indicate that the infection level gets reduced to zero for $\mathcal{T}_\circ \leq 1$, whereas the infection persists in the host body for $\mathcal{T}_1 > 1$. From the theoretical and numerical point of view, we concluded that Caputo derivatives have no influence on the stability of the equilibria.

As a future study, we seek to extend our proposed model to the case of the fractal-fractional system with the use of Adams-Bashforth numerical scheme [45, 46]. This special derivative is widely introduced in physics to explain various phenomena and laws. Also, the proposed model in this study can be enhanced by considering the effect of randomness. By using the approaches presented in [47, 48, 49, 50], we can simultaneously probe the effect of both memory and stochasticity on the viral dynamics. We will deal with it in our next work.

Declarations

Consent for publication

Not applicable.

Conflicts of interest

The authors declare that they have no conflict of interests.

Funding

Not applicable.

Author's contributions

M.N.: Conceptualization, Methodology, Writing-Original draft. Y.S.: Data Curation, Writing-Original draft, Software, Validation. A.Z.: Visualization, Investigation, Writing-Reviewing and Editing.

References

[1] Wang, S., & Zou, D. Global stability of in-host viral models with humoral immunity and intracellular delays. *Applied Mathematical Modelling*, 36(3), 1313-1322, (2012). [CrossRef]
[2] Wang, T., Hu, Z., Liao, F., & Ma, W. Global stability analysis for delayed virus infection model with general incidence rate and humoral immunity. *Mathematics and Computers in Simulation*, 89, 13-22, (2013). [CrossRef]
[3] Elaiw, A. M. Global stability analysis of humoral immunity virus dynamics model including latently infected cells. *Journal of biological dynamics*, 9(1), 215-228, (2015). [CrossRef]
[4] Dhar, M., Samaddar, S., & Bhattacharya, P. Modeling the effect of non-cytolytic immune response on viral infection dynamics in the presence of humoral immunity. *Nonlinear Dynamics*, 98(1), 637-655, (2019). [CrossRef]
[5] Hattaf, K., & Yousfi, N. Dynamics of SARS-CoV-2 infection model with two modes of transmission and immune response. *Math. Biosci. Eng*, 17(5), 5326-5340, (2020). [CrossRef]
[6] Wodarz, D., Christensen, J.P., & Thomsen, A.R. The importance of lytic and nonlytic immune responses in viral infections. *Trends in Immunology*, 23(4), 194-200, (2002). [CrossRef]
[7] Hollenberg, M.D., & Epstein, M. The innate immune response, microenvironment proteinases, and the COVID-19 pandemic: pathophysiologic mechanisms and emerging therapeutic targets. *Kidney International Supplements*, 12(1), 48-62, (2022). [CrossRef]
[8] Prakasha, D.G., Malagi, N.S., Veeresha, P., & Prasannakumara, B.C. An efficient computational technique for time-fractional Kaup-Kupershmidt equation. *Numerical Methods for Partial Differential Equations*, 37(2), 1299-1316, (2021). [CrossRef]
[9] Prakasha, D.G., Malagi, N.S., & Veeresha, P. New approach for fractional Schrödinger-Boussinesq equations with Mittag-Leffler kernel. *Mathematical Methods in the Applied Sciences*, 43(17), 9654-9670, (2020). [CrossRef]
[10] Baishya, C., & Veeresha, P. Laguerre polynomial-based operational matrix of integration for solving fractional differential equations with non-singular kernel. *Proceedings of the Royal Society A*, 477(2253), 20210438, (2021). [CrossRef]
[11] Fan, Y., Huang, X., Wang, Z., & Li, Y. Nonlinear dynamics and chaos in a simplified memristor-based fractional-order neural network with discontinuous memductance function. *Nonlinear Dynamics*, 93(2), 611-627, (2018). [CrossRef]
[12] Fan, Y., Huang, X., Wang, Z., & Li, Y. Global dissipativity and quasi-synchronization of asynchronous updating fractional-order memristor-based neural networks via interval matrix method. *Journal of the Franklin Institute*, 355(13), 5998-6025, (2018). [CrossRef]
[13] Agarwal, P., Baleanu, D., Chen, Y., Momani, S., & Machado, J. A. T. (Eds.). Fractional Calculus: ICFDA 2018, Amman, Jordan, July 16-18. Berlin, Germany: Springer, vol.303, (2019).
[14] Agarwal, P., Deniz, S., Jain, S., Alderremy, A.A., & Aly, S. A new analysis of a partial differential equation arising in biology and population genetics via semi analytical techniques. *Physica A: Statistical Mechanics and its Applications*, 542, 122769, (2020). [CrossRef]
[15] Song, L., Xu, S., & Yang, J. Dynamical models of happiness with fractional order. *Communications in Nonlinear Science and Numerical Simulation*, 15(3), 616-628, (2010). [CrossRef]
[16] Magin, L.R. Fractional calculus in Bioengineering, Part 1. *Critical Reviews in Biomedical Engineering*, 32(1), 1–104, (2004).
[17] Sadek, O., Sadek, L., Touhtouh, S., & Hajjaji, A. The mathematical fractional modeling of TiO–2 nanopowder synthesis by sol–gel method at low temperature, *Mathematical Modeling and Computing*, 9(3), 616–626, (2022). [CrossRef]
[18] Naik, P.A., Yavuz, M., Qureshi, S., Zu, J., & Townley, S. Modeling and analysis of COVID-19 epidemics with treatment in fractional derivatives using real data from Pakistan. *The European Physical Journal Plus*, 135(10), 1-42, (2020). [CrossRef]
[19] Özköse, F., Şenel, M.T., & Habbireeh, R. Fractional-order mathematical modelling of cancer cells-cancer stem cells-immune system interaction with chemotherapy. *Mathematical Modelling and Numerical Simulation with Applications*, 1(2), 67-83, (2021). [CrossRef]
[20] Özköse, F., Yavuz, M., Şenel, M.T., & Habbireeh, R. Fractional order modelling of omicron SARS-CoV-2 variant containing heart attack effect using real data from the United Kingdom. *Chaos, Solitons & Fractals*, 157, 111954, (2022). [CrossRef]
[21] Din, A., & Abidin, M.Z. Analysis of fractional-order vaccinated Hepatitis-B epidemic model with Mittag-Leffler kernels. *Mathematical Modelling and Numerical Simulation with Applications*, 2(2), 59-72, (2022). [CrossRef]

[22] Fatmawati, M.A.K., Bonyah, E., Hammouch, Z., & Shaiful, E.M. A mathematical model of tuberculosis (TB) transmission with children and adults groups: A fractional model. *AIMS Mathematics*, 5(4), 2813-2842, (2020). [CrossRef]
[23] M. Naim, F. Lahmidi, and A. Namir. *Global stability of a fractional order SIR epidemic model with double epidemic hypothesis and nonlinear incidence rate*. Communications in Mathematical Biology and Neuroscience, vol. 2020, Art. ID 38, 2020.
[24] Naim, M., Lahmidi, F., Namir, A., & Kouidere, A. Dynamics of an fractional SEIR epidemic model with infectivity in latent period and general nonlinear incidence rate. *Chaos, Solitons & Fractals*, 152, 111456, (2021). [CrossRef]
[25] Gholami, M., Ghaziani, R.K., & Eskandari, Z. Three-dimensional fractional system with the stability condition and chaos control. *Mathematical Modelling and Numerical Simulation with Applications*, 2(1), 41-47, (2022). [CrossRef]
[26] Zahid, A., Masood, S., Mubarik, S., & Din, A. An efficient application of scrambled response approach to estimate the population mean of the sensitive variables. *Mathematical Modelling and Numerical Simulation with Applications*, 2(3), 127-146, (2022). [CrossRef]
[27] Din, A., & Abidin, M.Z. Analysis of fractional-order vaccinated Hepatitis-B epidemic model with Mittag-Leffler kernels. *Mathematical Modelling and Numerical Simulation with Applications*, 2(2), 59-72, (2022). [CrossRef]
[28] Sene, N. Second-grade fluid with Newtonian heating under Caputo fractional derivative: Analytical investigations via Laplace transforms. *Mathematical Modelling and Numerical Simulation with Applications*, 2(1), 13-25, (2022). [CrossRef]
[29] Kumar, P., & Erturk, V.S. Dynamics of cholera disease by using two recent fractional numerical methods. *Mathematical Modelling and Numerical Simulation with Applications*, 1(2), 102-111, (2021). [CrossRef]
[30] Hammouch, Z., Yavuz, M., & Özdemir, N. Numerical solutions and synchronization of a variable-order fractional chaotic system. *Mathematical Modelling and Numerical Simulation with Applications*, 1(1), 11-23, (2021). [CrossRef]
[31] Daşbaşı, B. Stability analysis of an incommensurate fractional-order SIR model. *Mathematical Modelling and Numerical Simulation with Applications*, 1(1), (2021). [CrossRef]
[32] Carvalho, A.R., Pinto, C., & Baleanu, D. HIV/HCV coinfection model: a fractional-order perspective for the effect of the HIV viral load. *Advances in Difference Equations*, 2018(1), 1-22, (2018). [CrossRef]
[33] Naik, P.A., Zu, J., & Owolabi, K.M. Modeling the mechanics of viral kinetics under immune control during primary infection of HIV-1 with treatment in fractional order. *Physica A: Statistical Mechanics and its Applications*, 545, 123816, (2020). [CrossRef]
[34] Oustaloup, A., Levron, F., Victor, S., & Dugard, L. Non-integer (or fractional) power model to represent the complexity of a viral spreading: Application to the COVID-19. *Annual Reviews in Control*, 52, 523-542, (2021). [CrossRef]
[35] Podlubny. I. Fractional Differential Equations. *Academic Press, San Diego*, 1999.
[36] Odibat, Z.M., & Shawagfeh, N.T. Generalized Taylor's formula. *Applied Mathematics and Computation*, 186(1), 286-293, (2007). [CrossRef]
[37] Lin, W. Global existence theory and chaos control of fractional differential equations. *Journal of Mathematical Analysis and Applications*, 332(1), 709-726, (2007). [CrossRef]
[38] Li, H.L., Zhang, L., Hu, C., Jiang, Y.L., & Teng, Z. Dynamical analysis of a fractional-order predator-prey model incorporating a prey refuge. *Journal of Applied Mathematics and Computing*, 54(1), 435-449, (2017). [CrossRef]
[39] K. Diethelm. Analysis of Fractional Differential Equations: An Application-Oriented Exposition Using Differential Operators of Caputo Type. *Lecture Notes in Mathematics*, Springer-Verlag, Berlin, Germany, (2010, January).
[40] Ali, A., Ullah, S., & Khan, M.A. The impact of vaccination on the modeling of COVID-19 dynamics: a fractional order model. *Nonlinear Dynamics*, 1-20, (2022). [CrossRef]
[41] I. Petras. *Fractional-order Nonlinear Systems: Modeling Anlysis and Simulation*. Higher Education Press, Beijing, 2011.
[42] Vargas-De-León, C. Volterra-type Lyapunov functions for fractional-order epidemic systems. *Communications in Nonlinear Science and Numerical Simulation*, 24(1-3), 75-85, (2015). [CrossRef]
[43] Aguila-Camacho, N., Duarte-Mermoud, M.A., & Gallegos, J.A. Lyapunov functions for fractional order systems. *Communications in Nonlinear Science and Numerical Simulation*, 19(9), 2951-2957, (2014). [CrossRef]
[44] Huo, J., Zhao, H., & Zhu, L. The effect of vaccines on backward bifurcation in a fractional order HIV model. *Nonlinear Analysis: Real World Applications*, 26, 289-305, (2015). [CrossRef]
[45] Veeresha, P. A numerical approach to the coupled atmospheric ocean model using a fractional operator. *Mathematical Modelling and Numerical Simulation with Applications*, 1(1), 1-10, (2021). [CrossRef]
[46] Veeresha, P., Baskonus, H.M., & Gao, W. Strong interacting internal waves in rotating ocean: novel fractional approach. *Axioms*, 10(2), 123, (2021). [CrossRef]
[47] Kiouach, D., & Sabbar, Y. The long-time behavior of a stochastic SIR epidemic model with distributed delay and multidimensional Lévy jumps. *International Journal of Biomathematics*, 15(03), 2250004, (2022). [CrossRef]
[48] Kiouach, D., & Sabbar, Y. Threshold analysis of the stochastic Hepatitis B epidemic model with successful vaccination and Levy jumps. *In 2019 4th World Conference on Complex Systems (WCCS) (pp. 1-6)*, IEEE, (2019, April). [CrossRef]
[49] Sabbar, Y., Kiouach, D., Rajasekar, S.P., & El-Idrissi, S.E.A. The influence of quadratic Lévy noise on the dynamic of an SIC contagious illness model: New framework, critical comparison and an application to COVID-19 (SARS-CoV-2) case. *Chaos, Solitons & Fractals*, 159, 112110, (2022). [CrossRef]
[50] Kiouach, D., & Sabbar, Y. Modeling the impact of media intervention on controlling the diseases with stochastic perturbations. *AIP Conference Proceedings (Vol. 2074, No. 1, p. 020026)*, AIP Publishing LLC, (2019, February). [CrossRef]